AIAA Meeting Papers on Disc, January 1997
A9715327, AIAA Paper 97-0253

Analysis of scalar pdf models for turbulent non-premixed combustion

Graham M. Goldin
Georgia Inst. of Technology, Atlanta

Suresh Menon
Georgia Inst. of Technology, Atlanta

AIAA, Aerospace Sciences Meeting & Exhibit, 35th, Reno, NV, Jan. 6-9, 1997

Thermochemical scalar pdfs measured in nonpremixed hydrogen and methane turbulent jet flames are compared a priori with a sophisticated conventional assumed-shape pdf model, as well as a recently constructed pdf model. The constructed pdf, by incorporating the underlying physics of advection by all unsteady eddies, molecular diffusion and chemical reaction, displays consistent and substantial a priori improvement over the conventional assumed-shape pdf. In addition, the constructed pdf model is parameterized by considerably fewer lower moments, and in particular, first moments, promising affordable and accurate implementation in a moment equation solver. (Author)

ANALYSIS OF SCALAR PDF MODELS FOR TURBULENT NON-PREMIXED COMBUSTION

AIAA-97-0253

Graham M. Goldin*
Suresh Menon**

School of Aerospace Engineering
Georgia Institute of Technology

Abstract

Thermo-chemical scalar pdfs measured in non-premixed hydrogen and methane turbulent jet flames are compared *a-priori* with a sophisticated conventional assumed shape pdf model, as well as a recent constructed pdf model. The constructed pdf, by incorporating the underlying physics of advection by all unsteady eddies, molecular diffusion and chemical reaction, displays consistent and substantial *a-priori* improvement over the conventional assumed shape pdf. In addition, the constructed pdf model is parameterized by considerably fewer lower moments, and in particular, first moments, promising affordable and accurate implementation in a moment equation solver.

1. Introduction

In the moment equation approach for the computation of turbulent reacting flows, the governing Navier-Stokes (NS) equations are temporally (or ensemble) averaged to form the Reynolds Averaged Navier Stokes (RANS)[1] equations, or spatially averaged (filtered) to form the Large Eddy Simulation (LES)[2] equations. While averaging is required for tractable solution, unknown terms are introduced into the moment equations, and these require modeling. The accuracy and applicability of the solution, once numerical error is minimized, are determined by the quality of these models.

Two types of unknown terms can be identified in the moment equations. The first type are the turbulent convection terms, which are correlations with the velocity fluctuation, and are invariably closed by gradient diffusion assumptions. For example, in RANS, turbulent flux models range from the simplest zero order mixing length models, through first order closure such as $k-\varepsilon$, to Reynolds stress transport equations.

The second type of unknown terms are the scalar moments, and in particular, the mean chemical reaction rate. For general chemistry, the k-th species mean reaction rate, denoted $\overline{\dot{w}_k}$, is closed by convolution with the joint scalar probability density function (pdf) $P(\rho,T,Y_k)$, as

$$\overline{\dot{w}_k} = \int_0^\infty\int_0^\infty\int_0^1\cdots\int_0^1 \dot{w}_k(\rho,T,Y_k)\,P(\rho,T,Y_k)\,dY_1\cdots dY\,dT\,d\rho, \qquad (1)$$

where overbars denote unweighted averages, ρ is the density, T is the temperature, and Y_k is the k-th species mass fraction.

In turbulent flows, fluctuations arise as the scalars are advected by unsteady turbulent eddies, while simultaneously diffusing and reacting. The scalar pdf quantifies the relative time that the fluid spends at each composition (thermo-chemical) state, and scalar means, such as equation (1), are then a pdf weighted average over all allowable states. The pdf is, however, unknown, and must be modeled in terms of the available information, namely the solved lower moments.

Models for $P(\rho,T,Y_k)$, and in turn $\overline{\dot{w}_k}$, include the Laminar model, the Eddy-Break-Up (EBU)[3] model, the Eddy Dissipation Concept (EDC)[4] model and the assumed shape pdf model[1,5]. The Laminar model approximates the mean reaction rate by the expression for the instantaneous reaction rate evaluated at the mean scalars. This is equivalent to modeling the scalar pdf by Dirac Delta functions at the mean composition, and, by ignoring fluctuations, may be in error by several orders of magnitude. The EBU model offers some improvement by limiting the mean reaction rate to a mixing time scale, defined by the period for a large eddy turnover. The EDC model reasonably assumes that reaction occurs in fine scale structures, and approximates these as Perfectly Stirred Reactors. The problem with the EBU model, and to a lesser extent the EDC model, is the requirement for heuristic adjustment factors and non-universal calibration constants. An alternative to Laminar, EBU and EDC modeling is to assume a shape for the joint scalar pdf directly, which is usually attempted with combinations of Gaussian, Beta and Dirac Delta functions[1].

For the case of near-equilibrium chemistry, the analytical Gaussian-Beta-Delta assumed shape pdf is successful for the moment equation prediction of low Mach number, non-premixed combustion, where the chemistry can be reduced to a single scalar, such as the mixture fraction[1,6]. A similar reduction to a single scalar for premixed combustion is possible, but less satisfactory because the chemical source term cannot be eliminated[7]. However, the assumed shape pdf approach has severe limitations when extended to the moment equation solution of high speed and/or non-equilibrium reacting flows, where a large number of scalars are required to describe the chemistry, and the mean reaction rate is sensitive to the pdf shape due to the highly non-linear chemical kinetics[8].

A method to construct the joint scalar pdf instead of assuming its shape has recently been proposed[9,10,11]. The model accounts for the underlying unsteady small-scale turbulent dynamics and the distinct molecular processes, and is computationally feasible at high Re with complex kinetics. The objective of this work is to

* Graduate Research Assistant, Student Member AIAA., currently at Fluent, Inc.
** Associate Professor, Senior Member AIAA

compare conventional assumed shape pdfs and constructed pdfs against experimentally measured pdfs. The analysis is performed *a-priori* in that the lower moments, which are input to the assumed shape and constructed pdfs, are calculated from the experimental data, and not from moment transport equations. The *a-priori* analysis, while not predictive, remains a substantial model test for further implementation in predictive moment equation solvers.

The paper is structured as follows: Section 2 formulates a conventional assumed shape pdf. Section 3 provides an outline of the pdf construction model, which is formulated in section 4. Section 5 presents the results of the *a-priori* pdf comparison.

2. The conventional assumed shape pdf

A recent, and perhaps most advanced, assumed shape model for the full joint scalar pdf, $P(\rho,T,Y_k)$, has been proposed[5] and implemented[12,13,14] in a RANS simulation. This model, which is henceforth referred to as the conventional assumed shape pdf model, is formulated as,

$$P(\rho,T,Y_k)=\delta(\rho-\overline{\rho})\cdot P_G(T)\cdot P_\beta(Y_1,Y_2,\cdots,Y_N), \quad (2)$$

where $\delta(\rho-\overline{\rho})$ is a Dirac Delta distribution at the mean density, $P_G(T)$ is a normal (Gaussian) temperature distribution, and $P_\beta(Y_k)$ is a multi-variate Beta species distribution. The temperature is assumed to be statistically independent of the density and species, and normally distributed as,

$$P_G(T)=\frac{1}{\sqrt{2\pi\widetilde{T''^2}}}\exp\left(-\frac{(T-\tilde{T})^2}{2\widetilde{T''^2}}\right). \quad (3)$$

Note that density weighted (Favre) moments are denoted by overtildes. The assumed shape multi-variate species pdf is[5],

$$P_\beta(Y_1,Y_2,\cdots,Y_N)=\frac{\Gamma(\beta_1+\beta_2+\cdots\beta_N)}{\Gamma(\beta_1)\Gamma(\beta_2)\cdots\Gamma(\beta_N)} \cdot Y_1^{\beta_1-1}Y_2^{\beta_2-1}\cdots Y_N^{\beta_N-1}\,\delta(1-Y_1-Y_2-\cdots-Y_N), \quad (4)$$

where Γ is the Gamma function. The purpose of the Dirac Delta function in equation (4) is to exclude all points in Y_k composition space that do not satisfy $\sum Y_k=1$. The parameters $\beta_1,\beta_2,\cdots,\beta_N$ are specified as,

$$\beta_k=\tilde{Y}_k\left(\frac{1-S}{Q}-1\right), \quad (5)$$

where,

$$S=\sum_{k=1}^{N}\tilde{Y}_k^2, \qquad \text{and,} \qquad Q=\sum_{k=1}^{N}\widetilde{Y_k''^2}. \quad (6)$$

The assumed shape pdf requires N+3 lower moments to specify, where N is the number of species. These lower moments are the mean density ($\overline{\rho}$), the mean temperature and its variance ($\tilde{T}$ and $\widetilde{T''^2}$), N-1 mean species ($\tilde{Y}_k$) and the scalar energy (Q). A moment equation solution hence requires N+3 (modeled) transport equations for $\overline{\rho}$, $\tilde{T}$, $\widetilde{T''^2}$, $\tilde{Y}_k$ and Q.

In the following *a-priori* analysis, owing to the difficulty of graphically presenting multi-dimensional pdfs, marginal pdfs of $P(\rho,T,Y_k)$ are compared. The conventional marginal pdf of temperature is Gaussian, and the conventional marginal pdf of species Y_α, denoted $P_M(Y_\alpha)$ is[5],

$$P_M(Y_\alpha)=\frac{\Gamma(\beta_1+\beta_2+\cdots\beta_N)}{\Gamma(\beta_1)\Gamma(\beta_2)\cdots\Gamma(\beta_N)} \cdot Y_\alpha^{\beta_\alpha-1}(1-Y_\alpha)^{\beta_1+\cdots+\beta_{\alpha-1}+\beta_{\alpha+1}+\cdots+\beta_N-1}. \quad (7)$$

3. The LEM constructed pdf

A recently proposed pdf model constructs the joint scalar pdf as a function of its lower moments, as opposed to assuming its shape[9,10,11]. *The model approximates the scalar pdf in a general turbulent reacting flow by the pdf of scalars decaying in homogeneous turbulence, parameterized by an appropriate set of lower moments.*

The pdf construction model can be described by explaining the three major assumptions it is based upon.

The first assumption is that the critical features of the pdf of scalars decaying in homogeneous turbulence can be adequately parameterized by an appropriate set of lower moments. For example, the pdf of a single passive scalar decaying in homogeneous turbulence can be satisfactorily parameterized at all stages by its first two moments using a Beta function[15]. In this case the pdf shape, which in general requires an infinite set of lower moments to specify exactly, is closely specified by its mean and variance. However, since the mean remains constant during the decay, the pdf at any stage cannot be accurately parameterized by its mean value alone. Reducing the number of lower moment parameters represents an averaging of pdfs and, hence, a reduction in generality and accuracy. Clearly, the extension to multiple reacting scalars requires careful consideration to determine whether the pdf can be appropriately parameterized by a set of its lower moments.

The second assumption of the model is that the scalar distribution (pdf) in an arbitrary turbulent reacting flow can be approximated by the parameterized pdf of scalars decaying in homogeneous turbulence. Essentially, the assumption is made that the scalar distribution at a down-stream location in a general turbulent evolving flow is similar to the distribution that decayed after a certain time in homogeneous turbulence. That is, the history effects in the spatial evolution are assumed similar to the history effects of the scalar decay, for the moments not parameterized. The latter statement is important because if all (i.e., an infinite number of) lower moments are parameterized in the scalar decay, then a point in a general turbulent reacting flow with the identical lower moments will have the same pdf.

By assuming a generic geometry of homogeneous turbulence, non-homogeneous turbulence phenomena, such as large-scale coherent structures, cannot be captured. Also, scalar decay in homogeneous turbulence is sensitive to the initial scalar field. In this work, the initial condition is set as binary (a slab of fuel adjacent to a slab of oxidizer), in accordance with the non-premixed experimental comparison in section 5. For this reason, the pdf model, as presently implemented, may be considered to be limited to non-premixed RANS/LES applications. However, it is, in principle, possible to apply the same approach to premixed combustion, and perhaps construct a joint premixed and non-premixed turbulent combustion table. These assumptions appear somewhat severe and limiting, but must be weighed against the alternative of specifying the pdf shape, with its inherent difficulties and limitations. The accuracy, and cost, of the constructed and assumed shape pdfs are assessed in section 5.

This second assumption has great advantage for the moment equation approach because the expensive turbulence-chemistry interactions, implicit in the pdf, are determined off-line, and only once for a given chemistry. The pdf, or rather the mean chemical source term evaluated from equation (1), is generated and tabulated as a function of the lower moments. In a RANS/LES solution for these lower moments, the mean chemical source term is available directly from the table. This provides a significant computational saving as a RANS/LES integration of the stiff chemical kinetics would otherwise absorb a large fraction of moment equation solver run-time.

Accurate calculation of scalar decay in homogeneous turbulence can be obtained by Direct Numerical Simulation (DNS). However, despite the geometric simplicity of homogeneous turbulence, high *Re* DNS with complex chemistry remains computationally intractable. The third, and final, major assumption of the constructed pdf is that the statistical scalar distribution in a DNS of scalar decay in homogeneous turbulence can be well approximated by a corresponding Linear Eddy Model (LEM)[16,17] simulation. This is considered a good approximation because published LEM results have captured all critical features of mixing in homogeneous turbulence[17,18]. While the LEM has been validated against DNS, which is limited to moderate *Re*, its extension to higher turbulent *Re* is expected to be, if anything, more reliable because the LEM is based on high *Re* scaling laws.

4. The Linear Eddy Model

The LEM is a spatio-temporal Monte-Carlo simulation of the evolution of a scalar field in a turbulent flow[16,17]. All turbulence scales are resolved, in contrast to other mixing models such as gradient diffusion, so that turbulent advection and the separate processes of molecular diffusion and subsequent chemical reaction at the smallest scales are captured. This distinction is critical in combustion since chemical reaction proceeds at the molecular level when reactants (and heat) diffuse (and conduct) into contact. The rate of scalar diffusion, and hence chemical conversion for relatively fast chemistry, is strongly affected by the scalar gradients induced by the small scale turbulent motion.

The central LEM assumption is that the evolution of the scalar field at the small scales can be adequately captured by a simplified statistical description in one spatial dimension. Clearly, reduction to 1D entails geometric simplification, but allows affordable simulations at high *Re*, *Da* and *Sc*, a capability impossible in DNS.

As details of the LEM formulation are available in the literature[16,17], only a brief overview follows. Molecular diffusion and chemical reaction evolve deterministically from an initial specified scalar line by solution of the 1D species and temperature equations (with the convection term removed). The 1D species equation is,

$$\frac{\partial Y_k}{\partial t} = -\frac{1}{\rho}\frac{\partial}{\partial x}(\rho Y_k V_k) + \frac{\dot{w}_k}{\rho}, \qquad k = 1,2,\cdots N, \qquad (8)$$

where x is the LEM spatial co-ordinate and V_k is the diffusion velocity. V_k is modeled as a corrected Fick's law to satisfy $\sum Y_k V_k = 0$[19], viz.

$$Y_k V_k = -D_k \frac{\partial Y_k}{\partial x} + Y_k \sum_{j=1}^{N} D_j \frac{\partial Y_j}{\partial x}. \qquad (9)$$

Note that an arbitrary number of species may be simulated with general chemistry and general differential molecular diffusion co-efficients, D_k.

The *a-priori* analysis in this work is applied to low Mach number, near-adiabatic, (non-premixed), turbulent jet flames. Accordingly, the 1D LEM energy equation is

$$\rho\frac{\partial h}{\partial t} = -\frac{\partial q}{\partial x}, \qquad (10)$$

where h is the mixture averaged enthalpy, and q is 1D heat flux vector. Equation (10) is written equivalently as,

$$\frac{\partial T}{\partial t} = \frac{1}{\rho c_p}\frac{\partial}{\partial x}\left(\lambda\frac{\partial T}{\partial x}\right) - \frac{1}{c_p}\frac{\partial T}{\partial x}\sum_k c_{p_k} Y_k V_k - \frac{1}{\rho c_p}\sum_k h_k \dot{w}_k, \qquad (11)$$

where λ is the co-efficient of thermal conductivity, and $c_p = \sum Y_k c_{p_k}$ is the mixture averaged specific heat at constant pressure. All turbulent scales are resolved without averaging, and hence no modeling is required in equations (8) and (11).

The ingenious aspect of the LEM is the mechanism of advection by turbulent eddies, which is modeled in 1D as a stochastic re-arrangement of a portion of the scalar elements along the line. These instantaneous re-arrangement events, termed *triplet maps*, disrupt the continuous solution of the diffusion-reaction equations (8) and (11). Triplet mapping increases the scalar gradient, analogous to the effect of a similar sized micro-scale turbulent eddy on a physical scalar field. The element scalars are, however, unaltered, consistent with the picture that eddies transport fluid elements to nearby locations, and element scalars can only change by diffusion with neighboring elements and chemical reaction.

Since mappings always increase the scalar gradient, the 1D homogeneous turbulence LEM field may be considered as a time varying space curve aligned with the maximum scalar gradient. Periodic boundary conditions are implemented along the 1D LEM domain, and there is uniform spatial probability of an mapping event (eddy).

Inputs to the LEM simulation are the initial scalar field, and the largest (integral, L) and smallest (Kolmogorov, η) allowable eddy sizes. Governed by relations derived from inertial scaling laws, the field is stirred at fixed epochs by randomly sized eddies ranging in length from η to L, with great probability of near η sized mappings. Under the action of molecular diffusion and turbulent stirring, the scalar field decays to zero variance and the chemistry equilibrates. With increased turbulence (decreased L and η), frequent small scale stirrings induce steep scalar gradients, rapid scalar decay and increased non-equilibrium as the mixing time-scale approaches the chemical time-scale.

As the LEM velocity field is specified, acoustics cannot be discerned, and the LEM pressure field is assumed constant in space and time. The effect of heat release, which occurs at constant pressure, is twofold. The first is a change in the molecular transport co-efficients with the temperature increase. The second is due to the corresponding density decrease which conserves mass by volume expansion. The effect of heat release on turbulence is modeled by increasing L with the expanded domain, and increasing η in linear proportion, which assumes that the turbulent Reynolds number, $\mathrm{Re}_t = (L/\eta)^{4/3}$, remains constant with heat release. However, the turbulence is effectively decreased with increasing η because the small-scale scalar field straining is reduced. Since different LEM elements expand to different sizes, while triplet mapping requires equal sized elements, the scalar domain is re-gridded after heat release at the new required resolution, namely $\eta/6$. The overlapping scalar field in each LEM element after re-gridding is mixed without reaction. This spurious mixing is inconsequential since it occurs below the Batchelor length scale where scalar fluctuations are rapidly smoothed.

Without an ignition source, the non-premixed initial binary field diffuses to a uniform mixture of reactants at the initial reactant temperature. The present adiabatic ignition technique is to equilibrate a LEM element once it exceeds a certain 'degree of premixedness'. Denoting the initial (density weighted) volume averaged mole fractions of fuel and oxidizer in the domain as $\tilde{X}_F^o$ and $\tilde{X}_O^o$, an ignition mole fraction criterion is arbitrarily defined as,

$$X_{ig} = 0.5 \min(\tilde{X}_F^o, \tilde{X}_O^o). \tag{12}$$

An individual LEM element is 'ignited', that is equilibrated, when it satisfies the following 'premixed' criterion:

$$\begin{cases} X_F > X_{ig}, \\ X_O > X_{ig}. \\ T < 1500K. \end{cases} \tag{13}$$

Ignition events are numerous in the initial stages of a LEM simulation, but decrease as the scalar variance decays and the temperature rises.

The LEM pdf is constructed by performing LEM simulations over the entire range of allowable initial conditions (length of fuel slab relative to oxidizer slab), and turbulence (L and η). LEM pdfs with identical parameterizing lower moments are averaged over all simulations. Since the LEM is a Monte-Carlo simulation, pdfs are also averaged over a number of realizations to wash out stochastic error.

The LEM pdf in the following *a-priori* test is parameterized by the three mean species mass fractions $\tilde{Y}_F, \tilde{Y}_O$ and $\tilde{Y}_P$, where subscripts F, O and P denote fuel, oxidizer and product respectively. In RANS or LES applications, transport equations would be solved for these three lower moments only. All other moments, including first moments, that were not parameterized, can be obtained from the pdf. It is certainly possible, and perhaps more accurate, to parameterize the pdf by other moments such as $\tilde{T}$ or a mean radical mass fraction. The number and choice of parameterizing lower moments requires a careful analysis and is not attempted here. It is noted, however, that it may be beneficial to choose a moment whose accuracy is preferred, as a parameterizing lower moment. For example, if NO is of interest, it should be more accurate to solve a transport equation for $\tilde{Y}_{NO}$ and close $\overline{\dot{w}}_{NO}$ from the pdf, as opposed to obtaining $\tilde{Y}_{NO}$ from the scalar decay if moments other than $\tilde{Y}_{NO}$ are used to parameterize the pdf.

Hydrogen and methane fuels are examined in section 5. Despite the economy of the LEM, the pdf construction becomes expensive due to the large range of simulations and number of realizations. Accordingly, reduced four step mechanisms for hydrogen[20] and methane[21] combustion are implemented. The chemical kinetics and molecular transport properties are evaluated using the CHEMKIN II package[22]. Owing to the large diffusivity of H elements, and the corresponding LEM diffusion time-step limitations, the hydrogen flame pdfs are constructed from only 15 realizations, while the methane flame pdfs are constructed from 25 realizations. A moderate statistical error is implied, and pdf shapes are compared qualitatively. As the number of realizations increase, the LEM pdf shape becomes smoother, but its overall shape is not substantially changed.

5. *A priori* pdf analysis

An *a-priori* comparison of constructed, assumed shape and experimental pdfs follow. The experimental pdfs are obtained from simultaneous, time-resolved, species and temperature measurements in turbulent hydrogen[23] and methane[24] jet flames.

Two locations are selected in the hydrogen flame. The first location is the measured axial position nearest the nozzle (x/d=22.5) and the radial position closest to mean stochiometric mixture fraction (r/d=2.3). This is the anticipated measured location of greatest chemical non-equilibrium. Scalar pdfs at this location are presented in figure 1.

Figure 1(a) shows the marginal pdfs of molecular hydrogen for the experimental, LEM and multi-variate β pdfs. Both LEM

and assumed shape pdfs are accurate. Figure 1(b) is the marginal pdf of molecular oxygen, and the LEM pdf is much closer to the experimental pdf. Figure 1(c) plots the experimental, LEM and assumed shape marginal pdfs of *OH*. The LEM is in excellent agreement with measurements and captures a bimodal behavior. The pdf conformity implies that the experimental and LEM first moments, namely $\tilde{Y}_{OH}$, are close even though they were not matched in the LEM pdf construction. That is, the spatial evolution of the measured marginal *OH* pdf appears to be well approximated by the LEM temporal decay in homogeneous turbulence.

Figure 1(d) presents the experimental, LEM and Gaussian marginal temperature pdfs. Again, the LEM is superior to the Gaussian distribution, and this increased accuracy is substantial because the exponential dependence of reaction rates on temperature magnifies even small errors in the pdf. Note that the Gaussian pdf requires the experimental first two moments of temperature to specify, while the LEM pdf was constructed from the measured first moments $\tilde{Y}_{H_2}, \tilde{Y}_{O_2}$ and $\tilde{Y}_{H_2O}$ only. The large error in the assumed shape pdf is due to its inability to relate Favre averages and conventional (time) averages[12,13]. The fluid density drops by an order of magnitude when the temperature increases from $300K$ to $2300K$. The Gaussian pdf cannot account for the physics of density weighting, and weights all points in temperature space equally. The experimental pdf has a high peak at high temperature, but a corresponding smaller density weighting, so that in figure 1(d), the experimental weighted lower moments $\tilde{T}$ and $\widetilde{T''^2}$ are exactly equal to those of the unweighted assumed shape Gaussian pdf.

The second location in the hydrogen flame selected for *a-priori* analysis is the measured position furthest from the nozzle (x/d=180), and on the jet center-line (r/d=0). This location is the experimental visible flame tip, and corresponds to the other extreme where the chemistry is expected to be closest to equilibrium. Scalar pdfs at this location are presented in figure 2.

Figures 2(a) through 2(d) are the marginal pdfs of Y_{H_2}, Y_{OH}, Y_{O_2} and T, respectively. Far down-stream, most of the hydrogen is consumed, indicated by the 'spike' at $Y_{H_2} = 0$ in figure 2(a). Experimental non-zero values of Y_{H_2} are apparent, and the LEM is seen to capture this correctly. The hydroxl radical, *OH*, in figure 2(b) is similarly well predicted. The mixture fraction variance decays as x^{-2} in jet flames, and is small at down-stream locations. In accordance, all fluid elements are close to the mean mixture fraction and their densities are close to the mean density. The effect of density weighting is hence negligible at large axial distances from the nozzle, and since the scalar variance is small and the chemistry near equilibrium, the scalars are expected to be normally distributed. This is indeed the case in figures 2(c) and 2(d) where both the LEM and assumed shape marginal pdfs show reasonable agreement with the experimental marginal pdfs for oxygen and temperature respectively. Note that in figure 2(c) the multi-variate β pdf tends to a Gaussian distribution at small scalar variances.

A similar *a-priori* pdf analysis is performed for a turbulent methane-air jet flame[24] with a bulk jet velocity of $48m/s$. Experimental data was collected in visibly blue flame regions, implying small multi-phase (soot) and flame radiation effects. Pdfs are presented at a single flame location because the nearest (x/d=10) and furthest (x/d=50) locations are relatively close, and marginal pdfs at these extremes show insignificant differences. Again, the measured axial position nearest the nozzle (x/d=10), and the radial position closest to mean stochiometric mixture fraction (r/d=1.24) is selected for the *a-priori* analysis, which is the expected location of greatest non-equilibrium.

Figures 3(a) to 3(d) show experimental, LEM and assumed shape marginal pdfs of Y_{CH_4}, Y_{H_2O}, Y_{CO} and T, respectively. Again, the LEM displays closer agreement to the experimental distributions than the assumed shape pdf for all cases. The assumed shape marginal pdfs for Y_{CO} and T require the first moments $\tilde{Y}_{CO}$ and $\tilde{T}$, as well as the second moments Q and $\widetilde{T''^2}$, respectively, to specify, and are inaccurate due to the inability to account for density weighted averaging. The corresponding LEM marginal pdfs are not parameterized by, and hence not constrained to satisfy, $\tilde{Y}_{CO}$ and $\tilde{T}$. It is apparent that, based on the matched parameterizing lower moments $\tilde{Y}_{CH_4}, \tilde{Y}_{O_2}$ and $\tilde{Y}_{H_2O}$, the LEM pdf is capable of accurately predicting the marginal pdfs of Y_{CO} and T, and hence all lower Favre moments such as $\tilde{Y}_{CO}$ and $\tilde{T}$.

6. Conclusions and Summary

It is evident from figures 1, 2 and 3 that the LEM constructed pdf displays consistent and substantial improvement over the assumed shape pdf model. This accuracy is directly applicable to the moment equation solution of turbulent reacting flows. In such cases, required scalar lower moments such as $\overline{\dot{w}_k}$ and $\widetilde{RT}$ are evaluated from the pdf as in equation (1). The calculation of these multi-dimensional integrals is prohibitively expensive during run-time solution, and tabulation with run-time interpolation is necessary.

The conventional assumed shape pdf[5] under study for general $Y_k - T$ chemistry requires N+3 parameters to specify, where N is the number of chemical species. Beside the computational expense of solving N+3 transport equations in a moment equation simulation, the memory requirements and interpolation costs of a N+3 dimensional table are, if not intractable, exorbitantly expensive and impractical.

The conventional, assumed shape pdf approach has several other drawbacks. First, the assumed shape pdf does not consider the physical processes taking place. The actual pdf contains the information of scalar fluctuations at a point due to convection by all turbulence scales, molecular diffusion and chemical reaction, and one would expect the pdf to display some sensitivity to the turbulence dynamics (Re), the scalar molecular transport properties (Sc), as well as the chemical kinetics (Da). The conventional pdf model is incapable of directly incorporating Re-

Sc-Da effects, and the inclusion of complex flow phenomena, such as extinction, are precluded. Also, the assumption of statistical independence of all scalars is intuitively incorrect.

A second problem is the requirement for RANS/LES scalar variance (second moment) transport equations (e.g., $\widetilde{T''^2}$ and Q), which are difficult to model and a cause of inaccuracy[12,13]. A third drawback to the conventional assumed shape pdf model is the inability to relate Favre and conventional averages[12,13], which can lead to considerable error.

The Linear Eddy Model (LEM) pdf construction method approximates the thermo-chemical pdf in a general turbulent reacting flow by the pdf of thermo-chemical scalars decaying in homogeneous turbulence, parameterized by an appropriate set of lower moments. The assumption is made that the spatial evolution of the joint scalar pdf in a complex geometry combustor is similar to the scalar pdf that decayed from a binary initial condition in a homogeneous turbulent field, with the same suitable lower moments. This latter configuration is accurately modeled by the computationally affordable LEM, which resolves all turbulence scales, and can hence close the molecular processes of diffusion and chemical reaction exactly. The LEM pdf model is hence capable of incorporating *Re*, *Sc* and *Da* effects. The model has no adjustable constants or calibration factors, and although applied here to low Mach number, non-premixed combustion, is directly extendible to premixed and compressible flows.

The applicability and accuracy of the LEM pdf construction model is, of course, determined and limited by the assumptions it is based upon. In particular, by approximating the spatial evolution of the scalar pdf in an arbitrary turbulent reacting flow by the scalar decay from a binary initial condition in homogeneous turbulence, certain configuration specific phenomena cannot be discerned. The advantage gained is that the expensive turbulence-chemistry interactions can be decoupled from the RANS solution. In addition to this assumption, the pdf must be parameterized by a finite and small set of lower moments. Reducing the number of parameterizing lower moments represents an averaging of pdfs, and hence, a loss of generality. Finally, the constructed pdf contains the assumptions implicit in the LEM, for example constant pressure and the inability to account for the fluctuating pressure field.

These are big assumptions, but must be weighed against the alternative of assuming the pdf shape. This paper demonstrates the ability to accurately parameterize the LEM pdf by a small set of its lower moments, such as $\tilde{Y}_F$, $\tilde{Y}_O$ and $\tilde{Y}_P$. Although the LEM turbulent combustion table is expensive to construct, it is constructed only once for a given chemistry, and may subsequently be used indefinitely in moment equation solvers. In such RANS/LES solutions, transport equations are solved for the small number of parameterizing lower moments (e.g., $\tilde{Y}_F$, $\tilde{Y}_O$ and $\tilde{Y}_P$), which allows affordable table sizes and corresponding run-time interpolation costs. Further, the pdf may be parameterized by its first moments only, avoiding the difficulties, and errors induced, in modeling second moment (variance) transport equations.

Acknowledgments

The authors wish to thank Drs. R.S. Barlow and A.R. Masri for providing the experimental data. This work is supported in part by NASA Lewis Research Center, Office of Naval Research and Air Force Office of Scientific Research (under the Focused Research Initiative monitored by General Electric Aircraft Engine Company). This support is gratefully acknowledged.

References

1. Jones, W.P. and Whitelaw J.H. (1982) "Calculation Methods for Reacting Turbulent Flows: A Review", *Comb. and Flame* **48**, 1.
2. Menon, S., McMurtry, P.A. and Kerstein, A.R. (1993) "A Linear Eddy Mixing Model for LES of Turbulent Combustion", in *LES of Complex Engineering and Geophysical Flows* (Galerpin, B. and Orszag, S. ed.) Cambridge Univ. Press.
3. Spalding, D.B. (1977) "Development of the Eddy-Break-Up Model of Turbulent Combustion", *Sixteenth Symp. (Int.) on Comb.*, The Comb. Institute, 1627.
4. Magnussen, B.F. and Hjertager, B.H. (1976) "On Mathematical Modeling of Turbulent Combustion with Special Emphasis on Soot Formation and Combustion", *Sixteenth Symp. (Int.) on Comb.*, The Comb. Institute, 719.
5. Girimaji, S. S. "Assumed β -pdf Model for Turbulent Mixing: Validation and Extension to Multiple Scalar Mixing", *Comb. Sci. and Tech.* **78**, 177.
6. Bilger, R.W. (1980) "Turbulent Flows with Non-Premixed Reactants", in *Turbulent Reacting Flows* (Libby, P.A. and Williams, F.A. ed.), Springer-Verlag.
7. Williams, F.A. (1983) *Combustion Theory*, Second edition, Addison-Wesley.
8. Pope, S.B. (1990) "Computations of Turbulent Combustion: Progress and Challenges",*Twenty-Third Symp. (Int.) on Comb.*, The Comb. Institute, 591.
9. Goldin, G.M (1996) "A Linear Eddy Model for Steady-State Turbulent Combustion", PhD Thesis, Georgia Institute of Technology.
10. Goldin, G.M. and Menon, S. (1996) "A Pdf Construction Model for Non-premixed Turbulent Combustion", submitted to *Comb. Sci. and Tech.*
11. Goldin, G.M. and Menon, S. (1996) "A Linear Eddy Model for Steady-State Turbulent Combustion", *AIAA 96-0519.*
12. Baurle, R.A., Alexopoulos, G.A. and Hassan, H.A. (1994) "Assumed Joint Probability Density Function Approach for Supersonic Turbulent Combustion", *J. Prop. and Power*, **10**, 473.
13. Baurle, R.A., Hsu, A.T. and Hassan, H.A. (1995) "Assumed and Evolution Probability Density Functions in Supersonic Turbulent Combustion Calculations", *J. Prop. and Power* **10**, 473.
14. Narayan, J.R. (1994) "Effects of Turbulence-Chemistry Interactions in Compressible Reacting Flows", *AIAA-94-2311.*
15. Girimaji, S.S. (1991) "Assumed β -pdf Model for Turbulent Mixing: Validation and Extension to Multiple Scalar Mixing", *Comb. Sci. and Tech.***78**, 177.
16. Kerstein, A.R. (1988) "Linear Eddy Model of Turbulent Scalar Transport and Mixing", *Comb. Sci. and Tech.* **60**, *391.*

17. Kerstein, A.R. (1991) "Linear Eddy Modeling of Turbulent Transport. Part 6. Microstructure of Diffusive Scalar Mixing Fields", *J. Fluid Mech.* **231**, 361.
18. McMurtry, P.A., Gansuage, T.C., Kerstein, A.R. and Krueger, S.K. (1993) "Linear Eddy Simulations of Mixing in a Homogeneous Turbulent Flow", *Phys. Fluids A* **5**, 1023.
19. Coffee, T.P. and Heimerl, J.M. (1981) "Transport Algorithms for Premixed Laminar Steady-State Flames", *Comb. and Flame* **43**, 273.
20. Chen, J.Y. (1993) "Modeling of *NOx* Formation in Turbulent Jet Flames", *NAS3-26613.*
21. Seshadri, K. and Peters, N. (1990) "Reducing Mechanisms", *Reduced Kinetic Mechanisms and Asymptotic Approximations for Methane-Air Flames,* (Smooke M.D. ed.) Lecture Notes in Physics, Springer-Verlag.
22. Kee, R.J., Rupley, F.M., Miller, J.A. (1989) "CHEMKIN II: A Fortran Chemical Kinetics Package for the Analysis of Gas-Phase Chemical Kinetics", Sandia Rep. SAND 89-8009.
23. Barlow, R.S. and Carter, C.D. (1994) "Nitric Oxide Formation in Hydrogen Jet Flames", *Comb. and Flame* **97**, 261.
24. Masri, A.R., Bilger, R.W. and Dibble, R.W. (1988) "Turbulent Nonpremixed Flames of Methane Near Extinction: Probability Density Functions", *Comb. and Flame* **73**, 261.

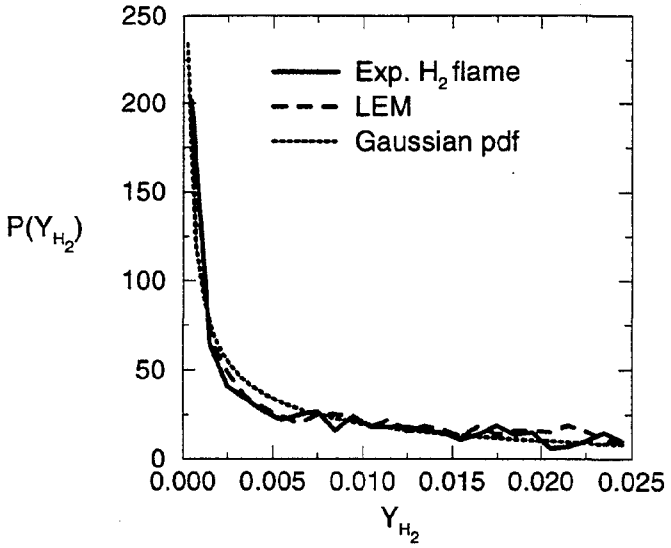

Fig. 1(a): Experimental, LEM constructed and multi-variate β marginal pdfs, $P(Y_{H_2})$, near the nozzle in a hydrogen-air flame.

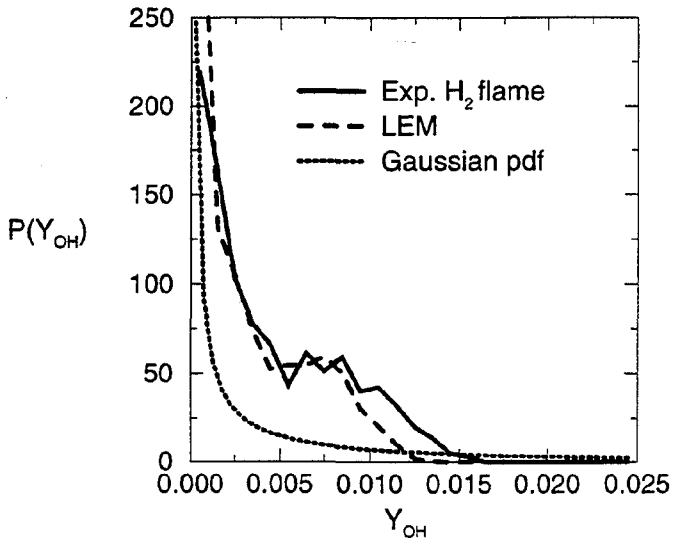

Fig. 1(c): Experimental, LEM constructed and multi-variate β marginal pdfs, $P(Y_{OH})$, near the nozzle in a hydrogen-air flame.

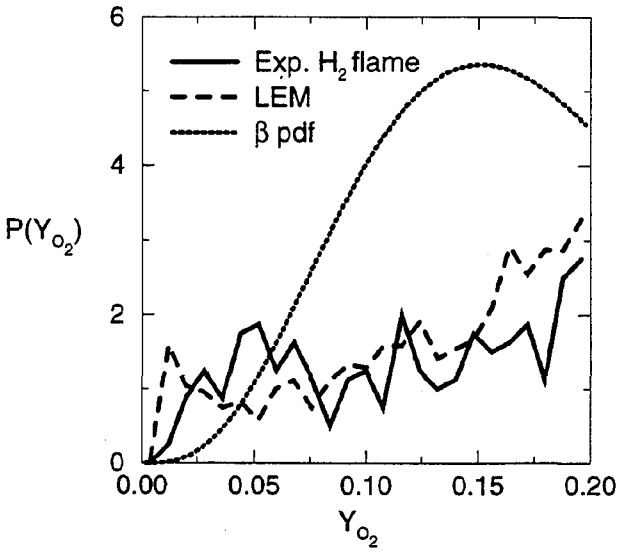

Fig. 1(b): Experimental, LEM constructed and multi-variate β marginal pdfs, $P(Y_{O_2})$, near the nozzle in a hydrogen-air flame.

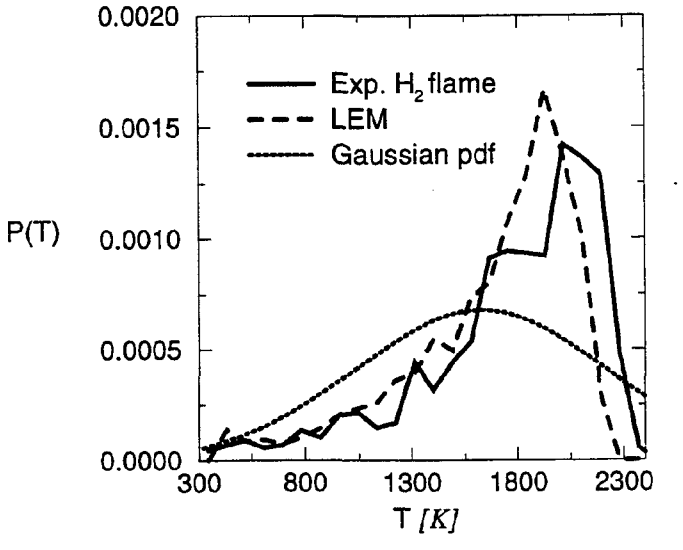

Fig. 1(d): Experimental, LEM constructed and Gaussian marginal pdfs, $P(T)$, near the nozzle in a hydrogen-air flame.

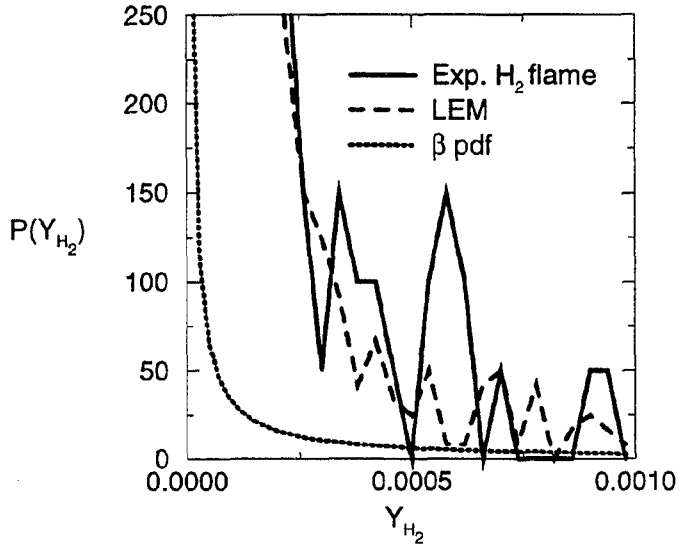

Fig. 2(a): Experimental, LEM constructed and multi-variate β marginal pdfs, $P(Y_{H_2})$, in the far field of a hydrogen-air flame.

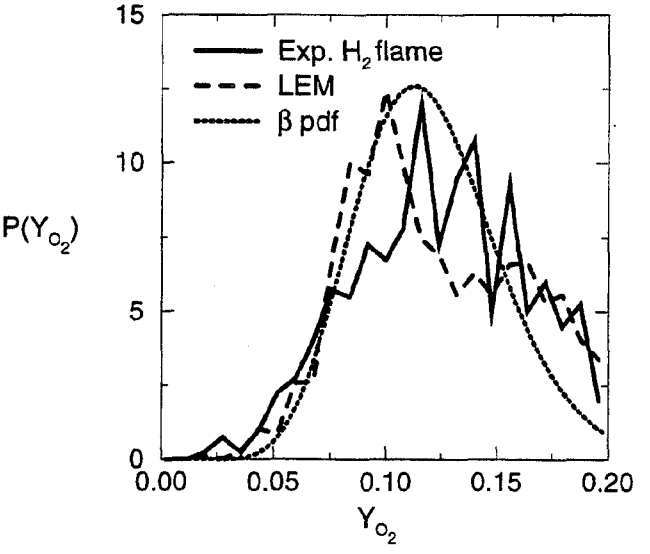

Fig. 2(c): Experimental, LEM constructed and multi-variate β marginal pdfs, $P(Y_{O_2})$, in the far field of a hydrogen-air flame.

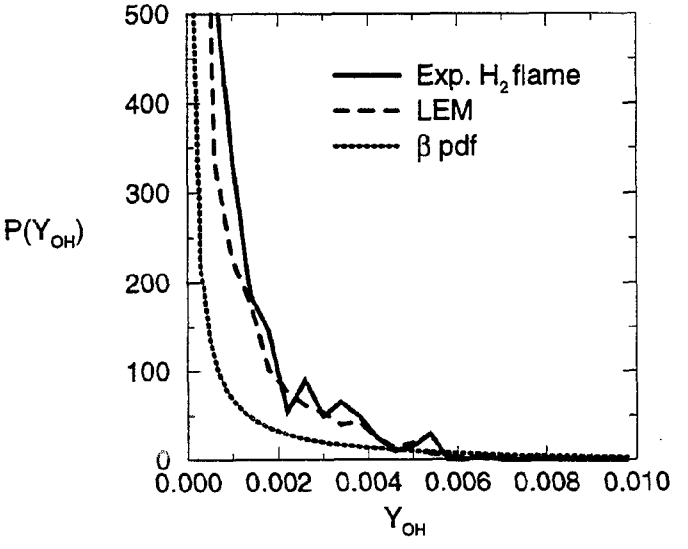

Fig. 2(b): Experimental, LEM constructed and multi-variate β marginal pdfs, $P(Y_{OH})$, in the far field of a hydrogen-air flame.

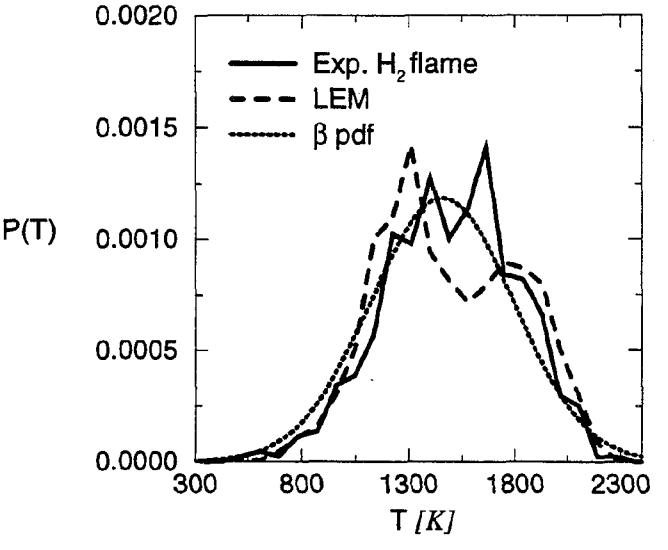

Fig. 2(d): Experimental, LEM constructed and Gaussian marginal pdfs, $P(T)$, in the far field of a hydrogen-air flame.

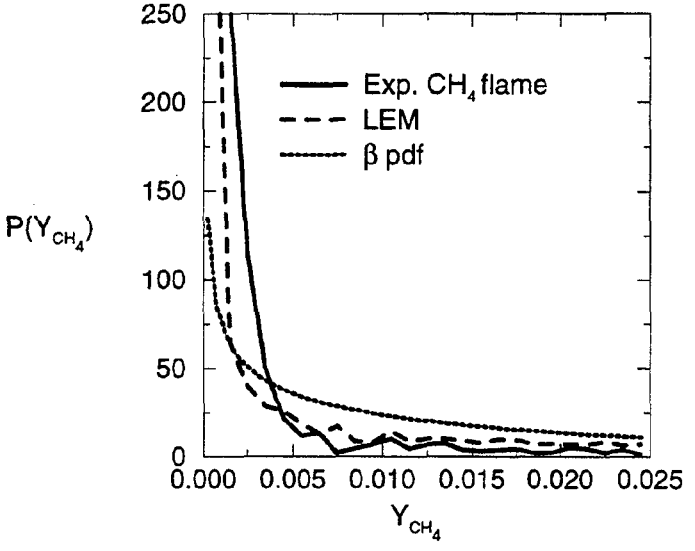

Fig. 3(a): Experimental, LEM constructed and multi-variate β marginal pdfs, $P(Y_{CH_4})$, near the nozzle in a methane-air flame.

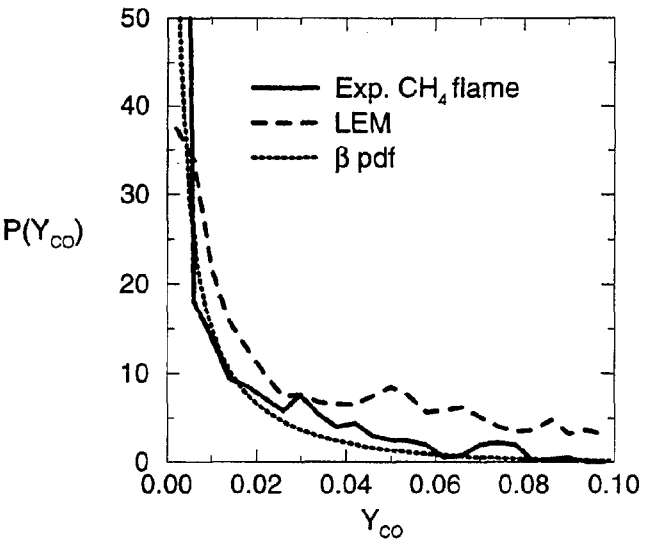

Fig. 3(c): Experimental, LEM constructed and multi-variate β marginal pdfs, $P(Y_{CO})$, near the nozzle in a methane-air flame.

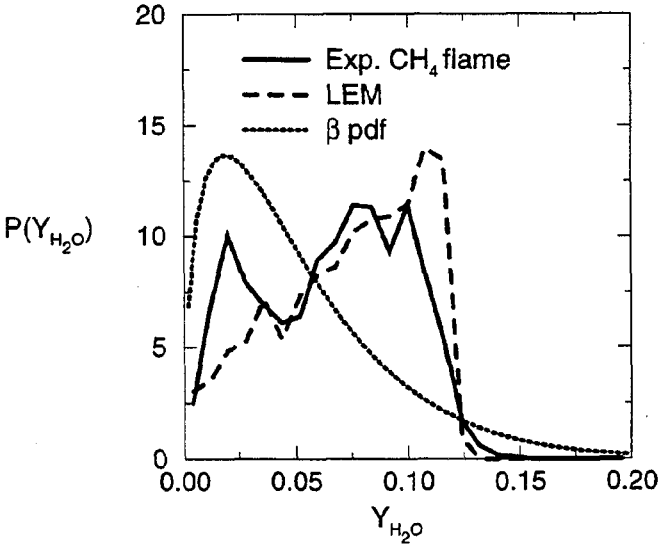

Fig. 3(b): Experimental, LEM constructed and multi-variate β marginal pdfs, $P(Y_{H_2O})$, near the nozzle in a methane-air flame.

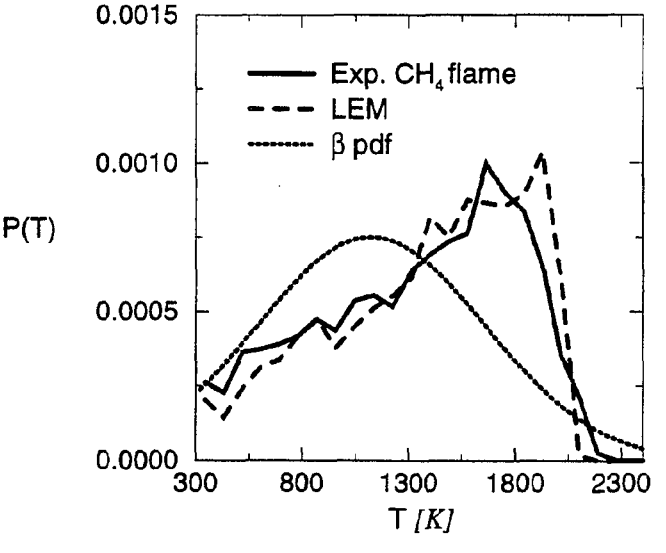

Fig. 3(d): Experimental, LEM constructed and Gaussian marginal pdfs, $P(T)$, near the nozzle in a methane-air flame.